Journal of Receptor, Ligand and Channel Research

Dovepress
open access to scientific and medical research

Open Access Full Text Article

ORIGINAL RESEARCH

# Interaction of recombinant and native $Ca_v2.3$ E-/R-type voltage-gated $Ca^{2+}$ channels with the molecular chaperone Hsp70

This article was published in the following Dove Press journal:
Journal of Receptor, Ligand and Channel Research
22 June 2011
Number of times this article has been viewed

Journal of Receptor, Ligand and Channel Research downloaded from https://www.dovepress.com/
For personal use only.

Kayalvizhi Radhakrishnan[1,2]
Andreas Krieger[1,2]
Etienne E Tevoufouet[1]
Gunnar PH Dietz[3,6]
Florian Nagel[4,6]
Matthias Bähr[5,6]
Jürgen Hescheler[1,2]
Toni Schneider[1,2]

[1]Institute of Neurophysiology, [2]Center of Molecular Medicine, University of Cologne, Köln, Germany; [3]Molecular Neurobiology, H Lundbeck A/S, Valby, Denmark; [4]Zentrum für Molekulare Neurobiologie, Forschergruppe Kramer, Hamburg; [5]Neurologische Universitätsklinik Göttingen, Göttingen, Germany; [6]DFG Research Center for Molecular Physiology of the Brain, University of Göttingen, Göttingen, Germany

**Abstract:** Cytosolic segments of membrane-bound voltage-gated $Ca^{2+}$ channels are targets for specific signaling complexes which regulate important physiological processes via soluble protein interaction partners. The molecular chaperone heat shock 70 kDa protein 1A (Hsp70) was identified as a binding partner for the II-III loop of the ion-conducting α1 subunit of the E-type voltage-gated $Ca^{2+}$ channel ($Ca_v2.3$) by mass spectrometry. To substantiate this finding further and to test its functional significance in vivo, two approaches were chosen. HEK-293 cells stably transfected with $Ca_v2.3$ were treated with a cell-permeable form of Hsp70 (Tat-Hsp70, Tat being a protein transduction domain of the "transactivator of transcription" from the human immunodeficiency virus) and analyzed by whole cell $Ca^{2+}$ current recordings. Tat-Hsp70 1 μM shifted the voltage-dependence of the inward currents to more hyperpolarized potentials. Further, the inactivation of transient inward $Ca^{2+}$ currents carried by $Ca_v2.3$ was slowed down. After isolation of hippocampal microsomes from control mice by ultracentrifugation, about 0.09% of total Hsp70 protein was bound to the microsomal fraction. Hsp70 binding to membranes was increased when kainate 20 mg/kg was injected intraperitoneally at concentrations which induced seizures and neurodegeneration in control mice. In $Ca_v2.3$-deficient mice, only mild seizures were observed after kainate injection, with no hippocampal neurodegeneration. Moreover, we observed no increase in Hsp70 binding to the membrane fraction of the isolated hippocampal microsomes, indicating that Hsp70 may be an important intermediate signaling partner for hippocampal neurodegeneration in $Ca_v2.3$(+/+) mice. Our results suggest that the $Ca_v2.3$ interaction partner, Hsp70, and its membrane association are important for understanding the molecular events in kainate-induced hippocampal neurodegeneration.

**Keywords:** protein–protein interaction, pharmacoresistant calcium current, R-type, kainate-induced epilepsy, neurodegeneration

## Introduction

Ten different genes encoding the ion-conducting α1-subunits of voltage-gated $Ca^{2+}$ channels (VDCCs) have been identified.[1–3] They are subdivided into three subfamilies, ie, $Ca_v1$ (L-type VGCCs), $Ca_v2$ (P-/Q-, N-, and E-/R-type VGCCs), and $Ca_v3$ (T-type VGCCs). The so-called "pharmacoresistant" E-/R-type VGCC has been inactivated in mice independently by different researchers, who analyzed the resulting complex phenotype in detail. The lifespan of $Ca_v2.3$-deficient mice was unchanged, but the physiological and pharmacological analyses revealed multiple abnormalities related to pain perception, synaptic plasticity, susceptibility to ischemic brain injury, sperm motility, cardiac arrhythmia, impaired insulin, glucagon and somatostatin release, and altered cocaine-induced behavior, as summarized recently.[3,4]

Correspondence: Toni Schneider
Institute of Neurophysiology, University of Cologne, Robert-Koch-Str 39, D-50931 Köln, Germany
Tel +49 22 1478 6946
Fax +49 22 1478 6965
Email toni.schneider@uni-koeln.de


© 2011 Radhakrishnan et al, publisher and licensee Dove Medical Press Ltd. This is an Open Access article which permits unrestricted noncommercial use, provided the original work is properly cited.

$Ca_v2.3$ $Ca^{2+}$ channels influence seizure susceptibility.[5] They exert antiepileptogenic effects on nonconvulsive absence seizures by modulating thalamocortical hyperoscillation.[6] However, for convulsive seizures induced by pentylenetetrazole and N-methyl-D-aspartate or by kainate injection, ictogenesis is reduced after ablation of *cacna1e*, the gene coding for $Ca_v2.3$, demonstrating resistance to limbic seizures and to cytotoxic cell death in $Ca_v2.3$-deficient mice.[7,8]

To understand the molecular mechanism of protection from kainate-induced neurodegeneration, we screened for protein interaction partners which may be putative candidates within a signaling pathway for selective hippocampal cell death. Using channel protein segments facing the cytosolic compartment, a biochemical approach demonstrated that the molecular chaperone, heat shock 70 kDa protein 1A (Hsp70), was tightly bound to the recombinant II–III loop when overexpressed in HEK-293 cells.[9]

Hsp70 is well-known to be upregulated by heat in both eukaryotic and prokaryotic cells.[10] Hsp70 expression is also triggered by other factors as soon as they generate adverse environmental conditions. Among these are increased levels of transition metal ions and sulfhydryl reagents, the presence of amino acid analogs, and glucose deprivation.[11] In the central nervous system, brain ischemia, traumatic injury, focal electrical stimulation, and kainate-induced seizures are accompanied by Hsp70 upregulation in both neuronal and glial cells.[12] Hsp70 immunopositive cells have been observed in the dentate gyrus region after kainate injection in rats. When insulin growth factor-1 was coadministered with kainate, less degeneration was observed, and fewer Hsp70 positive cells were detected.[13]

Not much has been reported in the literature about the interaction of ion channels and chaperones in the context of neuroprotection.[14,15] However, Hsp70 and additional molecular chaperones may provide first-line defense against neurodegeneration in animal models of a number of neurological disorders characterized by misfolded aggregation-prone proteins.[16] The molecular mechanism for the region-specific upregulation of Hsp70 is unknown, in spite of the fact that kainate-induced seizures in the hippocampus have been known for a decade.[17] In general terms, chaperone networks are crucial for sustained proteostasis,[18] which may be disturbed by kainate injection.

In the present study, we tested whether Hsp70, the newly identified interaction partner of the $Ca_v2.3$ II–III linker, may modulate $Ca_v2.3$-induced inward $Ca^{2+}$ currents, and whether it may be involved in kainate-induced seizures in mice. Therefore, we investigated the effect of the membrane-penetrating Tat-Hsp70 protein on channel kinetics in HEK-293 cells stably transfected with $Ca_v2.3$, and quantified the amount of membrane-bound Hsp70 and the change in Hsp70 binding to microsomal membranes in the hippocampus upon kainate injection in $Ca_v2.3$-deficient and control mice.

# Materials and methods

## Experimental animals

The mice were housed at a constant temperature (22–23°C), with light from 7 am to 7 pm and access to food and water ad libitum. All animal experimentation was conducted in accordance with accepted standards of humane animal care. The study was approved by the institutional committee on animal care, and was carried out in accordance with the European Communities Council Directive of November 24, 1986 (86/609/EEC).

The *cacna1E* gene was disrupted by deleting a region containing exon 2 in vivo on mating $Ca_v2.3$(fl/+) mice with *deleter* mice which express *Cre*-recombinase constitutively under the control of a cytomegalovirus promoter. After mating of $Ca_v2.3$(fl/+) and *deleter* mice, the offspring were genotyped by Southern blot analysis. In 20 of 83 pups (24%), exon 2 was deleted by *Cre*-mediated recombination. Heterozygous $Ca_v2.3$(+/−) mice were intercrossed to derive $Ca_v2.3$-deficient and $Ca_v2.3$(+/+) control mice, which were further inbred. Age-matched $Ca_v2.3$(+/+) mice were used as control animals throughout the experiment. Routine genotyping was performed by polymerase chain reaction on DNA from tail biopsies.

## Reagents

A FLAG (three-fold fusion tag consisting of eight amino acids $[DYKDDDDK]_3$)-tagged immunoprecipitation kit and other chemicals were obtained from Sigma (München, Germany). The anti-*myc* antibody was purchased from Invitrogen (Karlsruhe, Germany) and was diluted to1:5000 for Western blots as recommended by the manufacturer. The monoclonal anti-Hsp70 (Hsp72) antibody, C92F3A-5, was purchased from Assay Designs (Ann Arbor, MI). The bicistronic mammalian expression vector, pIRES-hrGFP-1a, was purchased from Stratagene (Amsterdam, the Netherlands).

## DNA vectors

The full length cDNA of $Ca_v2.3$ was cloned from fetal brain tissue,[19] and corresponds to the splice variant $Ca_v2.3d$ ($\alpha_{1Ed}$, GenBank Number L27745) which was subcloned into the pcDNA3 vector for transient or stable expression in

HEK-293 cells.[20] The full length II-III loop construct from the $Ca_v2.3$d-pcDNA3 vector was amplified with oligonucleotides as forward primers containing the NotI site and Kozak sequence, and with the reverse primer containing a Sal I site, as described in detail elsewhere.[9] The corresponding II–III loop of $Ca_v2.2$ was amplified from a vector containing human $Ca_v2.2$, kindly provided by Professor Shuji Kaneko (Kyoto, Japan) with the oligonucleotide NtypeNotI23fw (5′-ATG CGG CCG CCC ACC ATG GCC CAA GAG CTG ACC AAG-3′) as the forward primer, which translates into the amino acid AQELTK from human $Ca_v2.2$ (M94172), and with the oligonucleotide NtypeSalI23rvnew (5′-A CGT CGA CGA CCT CAT GGT CAC GAT GTA G-3′) as the reverse primer, which translates into the C-terminal sequence of VTMR(S).

A clone containing *hsp70* was purchased from the German Research Center for Genome Research (Berlin, Germany). The coding sequence for Hsp70 was amplified from clone IRALp962O0740 using the oligonucleotide hindhsp70fw as the forward primer (5′-CCC AAG CTT CCC GCC GCC GCC ATG GCC AAA GCC GCG GCG ATC-3′) and XhoIhsp70rev as the reverse primer (5′-AAC TCG AGC CAT CCA CCT CCT CAA TGG TAG G-3′). The cDNA fragment was digested with HindIII and XhoI, and subcloned into pcDNA3.1/myc-His. The polymerase chain reaction-amplified cDNA fragments and the resulting vector constructs were sequenced using standard methods.

## Transfection of HEK-293 cells for protein biochemistry

For immunoprecipitation experiments, HEK-293 cells were transfected using FuGENE HD (Roche Diagnostics, Mannheim, Germany) either with the vector pIRES-hrGFP-1a as the mock vector control or with the II-III loop from $Ca_v2.3$ or $Ca_v2.2$.

## Immunoprecipitation of FLAG-tagged proteins

The II–III loop and the C-terminal constructs were incorporated into the pIRES-hrGFP-1a vector in frame with the sequence for three consecutive FLAG-tags, (N-Asp-Tyr-Lys-Asp-Asp-Asp-Asp-Lys-C)$_3$. Soluble proteins were extracted using a lysis buffer consisting of Tris HCl 50 mM (pH 7.4), NaCl 150 mM, EDTA 1 mM, and Triton X-100 1% (v/v). The FLAG-tagged proteins were isolated by affinity chromatography according to the instructions of the manufacturer (FLAGIPT-1, Sigma, Munich, Germany). All steps were performed at 4°C.

## Expression and purification of Tat-Hsp70

The Tat-Hsp70 protein was generated as outlined elsewhere.[21,22] The rat Hsp70.1 cDNA was cloned into a pTat-hemagglutinin expression vector according to a method already described,[22] overexpressed in Escherichia coli, and purified by metal-affinity chromatography using Ni-tris-carboxymethyl-ethylene-diamine (Macherey-Nagel, Düren, Germany). After stepwise elution with increasing concentrations of imidazole, salts and imidazole were removed by size exclusion chromatography. Protein purity was assessed via sodium dodecyl sulfate gel electrophoresis and subsequent Coomassie staining.

## Western blotting

HEK-293 cells were grown as previously described.[23] Proteins were separated by polyacrylamide gel electrophoresis according to standard protocols and were immunoblotted as reported elsewhere.[23] The ECL detection kit used was purchased from GE Healthcare (Freiburg, Germany).

## Voltage clamp recordings

Membrane currents from HEK-293 cells stably transfected with $Ca_v2.3$ (HEK-2C6 cells) were recorded in the tight-seal whole cell configuration using the patch clamp technique,[24,25] with $Ca^{2+}$ 5 mM as the charge carrier in the external solution. HEK-2C6 cells were voltage-clamped at –90 mV using the EPC-9 patch clamp amplifier (HEKA Elektronik, Lambrecht, Germany). Cell capacitance varied between 12 pF and 20 pF. Currents were filtered with a three-pole analog Bessel filter set as a cutoff (–3 dB) at 10 kHz. Patch clamp electrodes were pulled from thick wall borosilicate glass using a Sutter P97 horizontal puller (Sutter Instrument Company, Novato, CA). The resistance of the pipette tip was in the range of 2–7 mΩ when filled with the electrode solution containing CsCl 130 mM, oxaloacetate 5 mM, creatine 5 mM, pyruvate 5 mM, EDTA 0.02 mM, 10 mM HEPES adjusted to pH 7.35 with CsOH (osmolality 272 mOsmol/kg). The bath solution contained $CaCl_2$ 5 mM, N-methylglucamine 160 mM, HEPES 10 mM, and KCl 5 mM, at pH 7.35 with HCl (osmolality 305–320 mOsmol/kg). All experiments were performed at room temperature (22–24°C). Gravitation-driven perfusion was performed using a precision perfusion controlling system and a round cover-slip chamber (RC-25, 13 mm; Warner Instruments, Hamden, CT).

## Data analysis and curve fitting

Current amplitudes and kinetics were recorded as reported previously.[24] Inactivation kinetics of the currents were estimated by fitting the decaying part of the current traces with

the equation: $I(t) = a_o + a_1*\exp(-(t - x)/\tau_1)$. The data are expressed as mean ± standard error of the mean, and n is the number of cells used. Statistical significance was analyzed using Student's *t*-test, and levels of $P < 0.05$ were considered to be statistically significant.

# Results

## Coimmunoprecipitation of human Hsp70 with II–III loops of $Ca_v2.2$ and $Ca_v2.3$

Expression of the FLAG-tagged II-III linker with myc-tagged human Hsp70 led to coimmunoprecipitation of myc-tagged Hsp70 by FLAG-IP (Figure 1A, lane 1) as reported recently.[9] Under similar conditions, the II-III loop of the human $Ca_v2.2$ (N-type) $Ca^{2+}$ channel also immunoprecipitated with myc-tagged Hsp70 (Figure 1A, lane 3). However, no specific immunoprecipitation was observed with the C-terminus of $Ca_v2.3$ (Figure 1A, lane 5 vs lane 7), although sufficient Hsp70 protein was expressed (compare supernatants from both batches, Figure 1A, lane 6 vs lane 8), assuming that the cytosolic II–III linkers rather than the C-terminus may be a common target for membrane-bound Hsp70, at least for human E-/R-type and N-type voltage-gated $Ca^{2+}$ channels.

In previous studies, 15-deoxyspergualin, the synthetic analog of spergualin, was used in a retina model to test its functional effects on E-/R-type channel-mediated gamma aminobutyric acid release.[9,26] To understand the 15-deoxyspergualin-mediated physiological effects, we tested the hypothesis that 15-deoxyspergualin may interfere directly with Hsp70 binding to the II–III loop. Immunoprecipitation of Hsp70 with the II–III loop of $Ca_v2.3$ was tested in two separate experiments in the presence of increasing concentrations of 15-deoxyspergualin (Figure 1B). Similar amounts of II–III loop were precipitated at all concentrations of 15-deoxyspergualin tested (Figure 1B, upper panels with anti-FLAG as the primary antibody [lanes 1, 3, 5, 7, 9, 11]). However, the amount of Hsp70 was slightly reduced (see arrowhead in Figure 1B) when 15-deoxyspergualin 100 μM was present (Figure 1B, compare lane 11 with lanes 7 and 9), leading to the conclusion that direct drug–protein competition may not be the major mechanism explaining the functional effects of 15-deoxyspergualin on retinal signaling.

## Tat-Hsp70 affects kinetics of HEK-293 (2C6) cells expressing $Ca_v2.3$

Hsp70 is too large to pass freely across biological membranes, but fusion of the Hsp70 protein with the protein transduction domain, Tat, enables translocation of this protein across the cellular membrane, including across the blood–brain barrier.[27] To test if Tat-mediated Hsp70 translocation might influence $Ca_v2.3$-carried $Ca^{2+}$ currents, HEK-293 cells stably transfected with $Ca_v2.3$ were preincubated with highly purified Tat-Hsp70 1 μM overnight.[27] The voltage dependence of inward currents with $Ca^{2+}$ as a charge carrier was compared for control cells and for cells preincubated with Tat-Hsp70 (Figure 2A). The threshold of peak $I_{Ca}$ and the potential of half-maximal activation were shifted by about 7 mV to more negative potentials (control cells $V_{0.5} = 5.1 \pm 2.9$ mV, n = 9; cells preincubated with Tat-Hsp70 $V_{0.5} = -2.1 \pm 1.4$ mV, n = 11, $P = 0.029$). The maximal slope conductance was 1.63 and 1.62 nA/V for control and cells preincubated with Tat-Hsp70, respectively. These results demonstrate that Tat-Hsp70 shifts the voltage dependence of activation to more hyperpolarized potentials, which could influence the excitability of a cell in vivo.

The overall current density was not changed by the application of Tat-Hsp70. The mean inward current was 16.7 ± 2.0 pA/pF in control cells (n = 12), and increased slightly without reaching the level of significance in cells pretreated with Tat-Hsp70 (18.9 ± 1.4 pA/pF, n = 15, Figure 2B).

Inactivation of $Ca_v2.3$-carried inward currents is best fitted by two exponentials,[28] given that the fast and slow components of inactivation are modulated by $Ca^{2+}$ differently.[24] Therefore, we analyzed fast and slow inactivation by fitting the inactivation part of the current traces with two exponentials and plotted the inactivation time constants for early and later recorded sweeps (Figures 2C and 2D). Fast inactivation time constants were 49–72 milliseconds for control cells and 46–57 milliseconds for cells pretreated with Tat-Hsp70. The slow inactivation time constants were 92–97 milliseconds for control cells and 95–97 milliseconds for cells preincubated with Tat-Hsp70. No significant difference was found between the two types of cells. Therefore, we normalized the current traces and superimposed the means from the control cells and cells pretreated with Tat-Hsp70 (Figure 2E). Cells preincubated with Tat-Hsp70 showed a slowing of inactivation, which reached a level of statistical significance 100 milliseconds after depolarization of the cells (see label in Figure 2E).

Comparison of the voltage-dependence of steady-state inactivation for $Ca_v2.3$ currents in control cells and in cells preincubated with Tat-Hsp70 showed a shift in the voltage of half-maximal inactivation to more hyperpolarized potentials for the pretreated cells ($P = 0.07$). The voltage of half-maximal inactivation was −17.0 ± 4.9 mV for control cells (n = 4) and −28.4 ± 2.9 mV for cells preincubated with Tat-Hsp70 (n = 9, Figure 2F). No difference was observed for fractional recovery after short-term inactivation (Figure 2G).

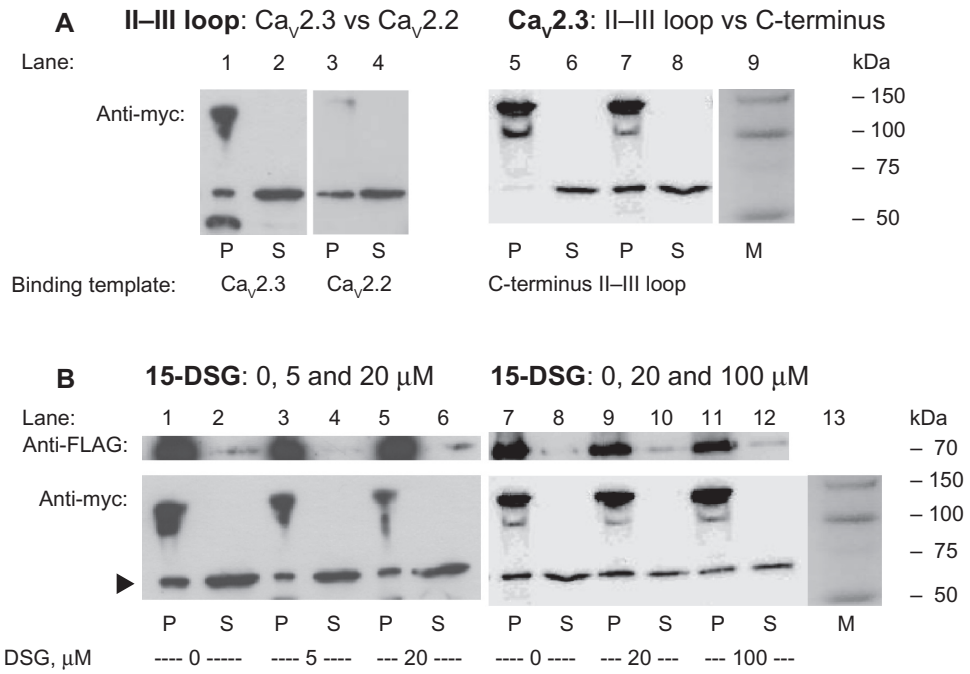


**Figure 1** Coimmunoprecipitation of FLAG-tagged cytosolic channel domains and c-myc-tagged Hsp70 protein. **A**) After overexpression of the cytosolic II–III linker from $Ca_v2.2$ (N-type VGCC) and $Ca_v2.3$ (E-/R-type VGCC) soluble proteins from transfected HEK-293 cells were extracted and immunoprecipitated by anti-FLAG-linked beads. The adsorbed proteins were eluted by a sodium dodecyl sulfate-denaturing buffer and separated by sodium dodecyl sulfate polyacrylamide gel electrophoresis (the precipitated fractions are labeled as "P", and the soluble fraction before immunoabsorption as "S"). After Western blotting, anti-c-myc was used as the primary antibody. In separate experiments, either the cytosolic linkers between domain II and III from $Ca_v2.2$ (lanes 3 and 4) or from $Ca_v2.3$ (lanes 1 and 2) were expressed in HEK-293 cells. Furthermore, the overexpressed C-terminus from $Ca_v2.3$ (lanes 5 and 6) was compared with the $Ca_v2.3$ II–III loop (lanes 7 and 8). Note that only nonspecific proteins with molecular sizes larger than 100 kDa were immunoprecipitated when the C-terminus was expressed as the FLAG-template, but not myc-Hsp70 protein (compare lane 5 and lane 7, arrowhead). **B**) After overexpression of the cytosolic II–III linker from $Ca_v2.3$ (E-/R-type VGCC) soluble proteins from myc-Hsp70-transfected HEK-293 cells were extracted and immunoprecipitated by anti-FLAG-linked beads in the absence (lanes 1 and 2 vs lanes 7 and 8) and in the presence of 15-DSG 5 μM (lanes 3 and 4), 15-DSG 20 μM (lanes 5 and 6 vs lanes 9 and 10), and 15-DSG 100 μM (lanes 11 and 12). In the upper half, the amount of II–III linker expressed is visualized by anti-FLAG staining of the precipitate ("P") and the supernatant before loading ("S"). Note, the anti-myc-positive protein is only slightly reduced in the presence of the highest concentration of 15-DSG used (lane 11), where the soluble fraction may also contain less expressed Hsp70 (lane 12).
**Abbreviations:** 15-DSG, 15-deoxyspergualin; Hsp70, heat shock 70 kDa protein 1A; VGCC, voltage-gated $Ca^{2+}$ channel.

In conclusion, Hsp70 affects $Ca_v2.3$-carried inward currents with $Ca^{2+}$ as the charge carrier. Activation and inactivation are shifted towards more negative potentials.

## Hsp70 binding to microsomal membranes in controls and $Ca_v2.3$-deficient mice

Hsp70 expression is increased up to three-fold within 1 day after intracerebroventricular injection of kainate into the adult rat hippocampus.[12] Such cell-specific expression of Hsp70 in hippocampal neurons as well as in glial cells is known for rats[17,29] as well as for mice, in which kainate generates gamma oscillations via the glutamate receptor subunits, GluIR5 and GluR6.[30] Upon administration of kainate 30 mg/kg intraperitoneally to $Ca_v2.3$-deficient mice, seizure architecture altered, and resistance to limbic seizures was increased compared with control mice, although no difference in electroencephalographic hippocampal seizure activity between either genotype could be detected at this suprathreshold dosage. Furthermore, histochemical analysis within the hippocampus revealed excitotoxic effects after kainate administration only for $Ca_v2.3$ controls but not for $Ca_v2.3$-deficient mice.[8] Because Hsp70 was identified as a tightly bound interaction partner of $Ca_v2.3$,[9] similar kainate injection experiments were repeated at 20 mg/kg instead of 30 mg/kg[8] to reduce the number of mice reaching a stage of maximum generalized seizure activity and to keep a sufficient number of control mice alive. Hsp70 expression was compared for both genotypes before and after kainate injection. Because Hsp70 binds to the membrane-integrated channel via the cytosolic II–III linker, membrane-bound Hsp70 was taken as the readout for our experiments, and was quantified after sodium dodecyl sulfate gel electrophoresis by Western blotting and scanning densitometry of the immunostained Hsp70 bands (Figure 3A). After homogenization of the murine hippocampal tissues, Hsp70 was precipitated by ultracentrifugation, assuming that this molecular chaperone is bound to membrane proteins from the microsomal fraction. In quantitative terms, 1.2% of the total protein homogenized was detected after ultracentrifugation in the microsomal fraction. However, for the immunostained Hsp70, only 0.09% of the initial Hsp70 protein was bound to the membrane fraction.

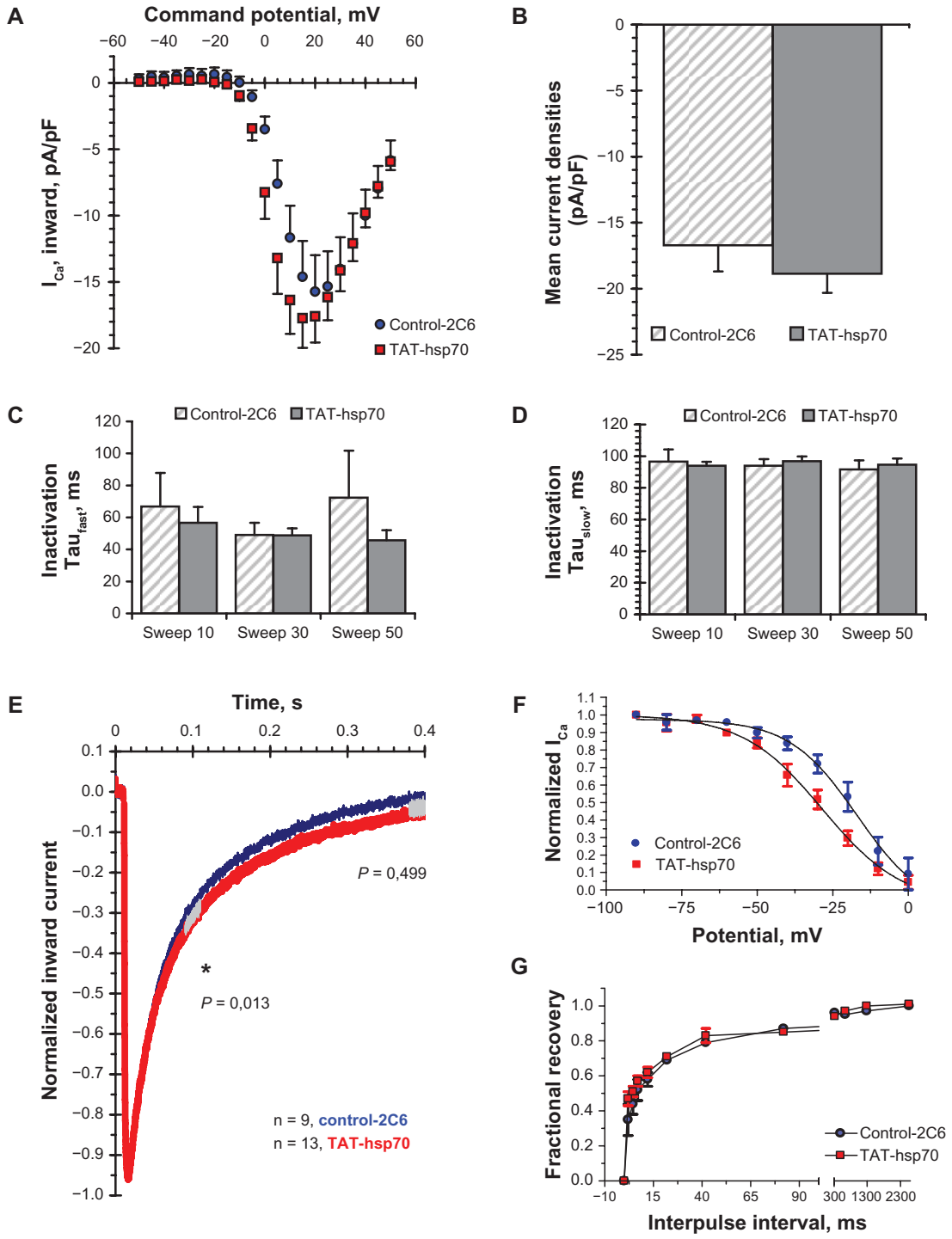


**Figure 2** Hsp70 affects the threshold for activation and the inactivation kinetics of $Ca_v2.3$-mediated inward currents. Inward $Ca^{2+}$ currents were recorded with a $Ca^{2+}$ concentration of 5 mM. **A**) Pooled current-voltage relationships determined in control cells (•, n = 9) or in cells preincubated in Tat-Hsp70 1 μM overnight (■, n = 11). The holding potential was –50 mV to +50 mV. **B**) Maximal peak inward current for control cells (open bar, n = 12) and for cells preincubated in Tat-Hsp70 1 μM overnight (filled bar, n = 15). **C**) Mean values of the fast inactivation time constant ($tau_{fast}$) after 10, 30, and 50 sweeps. Currents were evoked by 400 millisecond depolarizations from –90 mV to +30 mV. **D**) Mean values for the slow inactivation time constants from currents as recorded in panel C. **E**) Superpositions of mean current traces after normalization from control cells (n = 9) and cells preincubated with Tat-Hsp70 (n = 13). Note, the preincubation of HEK-293 (2C6) cells with Tat-Hsp70 slows down inactivation slightly, which is significant for the time window of 100 milliseconds as indicated ($P = 0.013$). The regions for testing significance were labeled by the plotted scatter in this time window (at 100 and 400 milliseconds). **F**) Steady-state inactivation of $Ca_v2.3$-carried $Ca^{2+}$ currents were recorded at –90 mV after a 5-second prepulse applied from –90 mV to + 20 mV. The holding potential was –90 mV. Data were filtered at 10 kHz. Under these conditions, the whole cell current inactivated nearly completely. **G**) Mean fractional recovery from short-term inactivation under control conditions (•; n = 4), and after preincubation with Tat-Hsp70 (■; n = 5).

**Abbreviations:** TAT, protein transduction domain of the "transactivator of transcription" from the human immunodeficiency virus; Hsp70, heat shock 70 kDa protein 1A.

To increase the accuracy of Hsp70 quantification (Figure 3B), the pixel density of the immunopositive bands was normalized by calculating the ratio of the 70 kDa positive band (Hsp70) divided by the pixel density of a nonspecific 100 kDa band (Figure 3A, Table 1). Relative numbers for $Ca_v2.3$-deficient mice (0.50 ± 0.01, n = 10 lanes from five Western blots of two membrane batches) did not differ significantly from the corresponding numbers for $Ca_v2.3$ control animals (0.42 ± 0.06, n = 10, $P = 0.45$). After kainate injection, the amount of Hsp70 bound to $Ca_v2.3$-deficient microsomes (0.64 ± 0.09, n = 13,

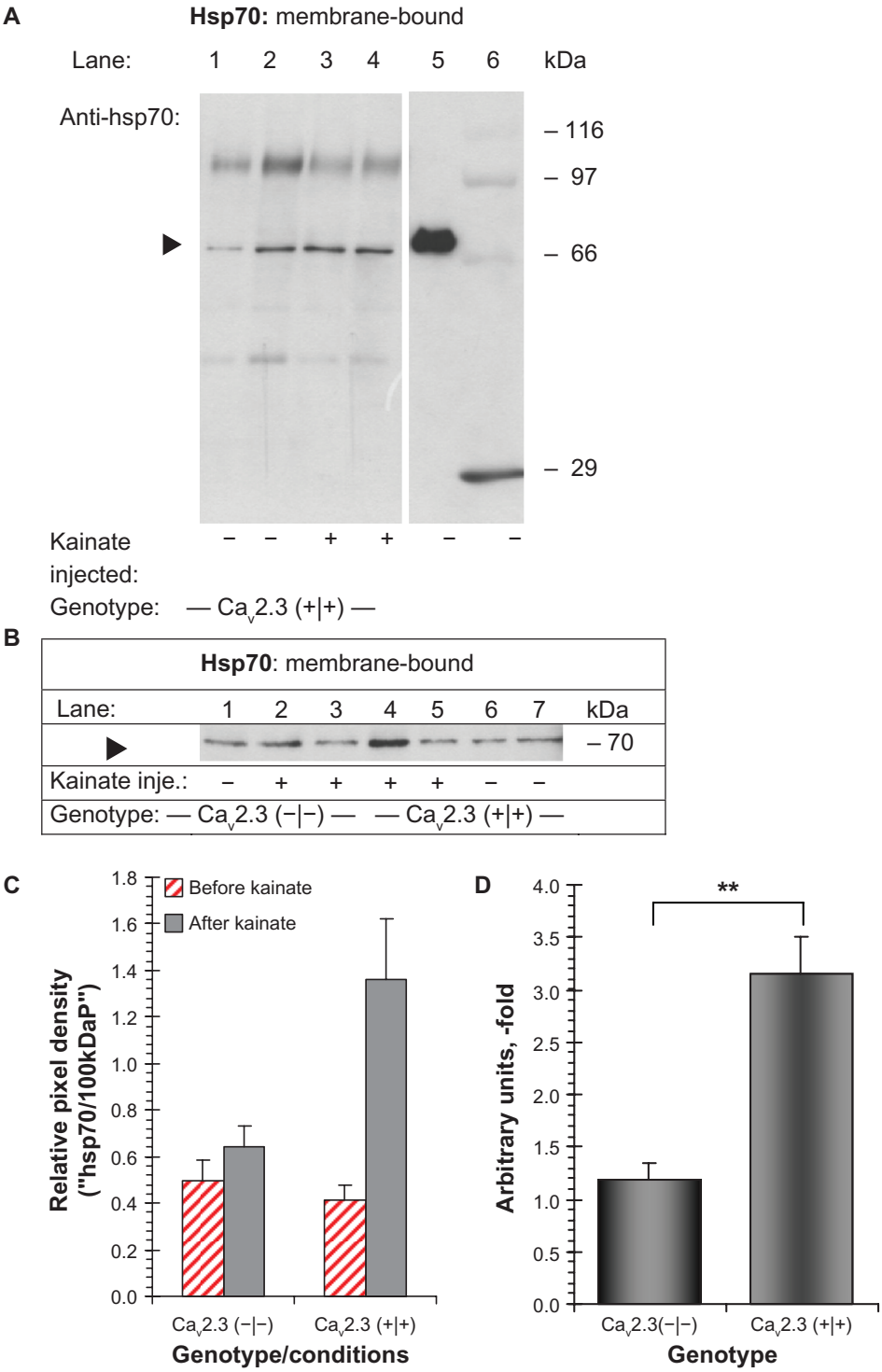


**Figure 3** (*Continued*)

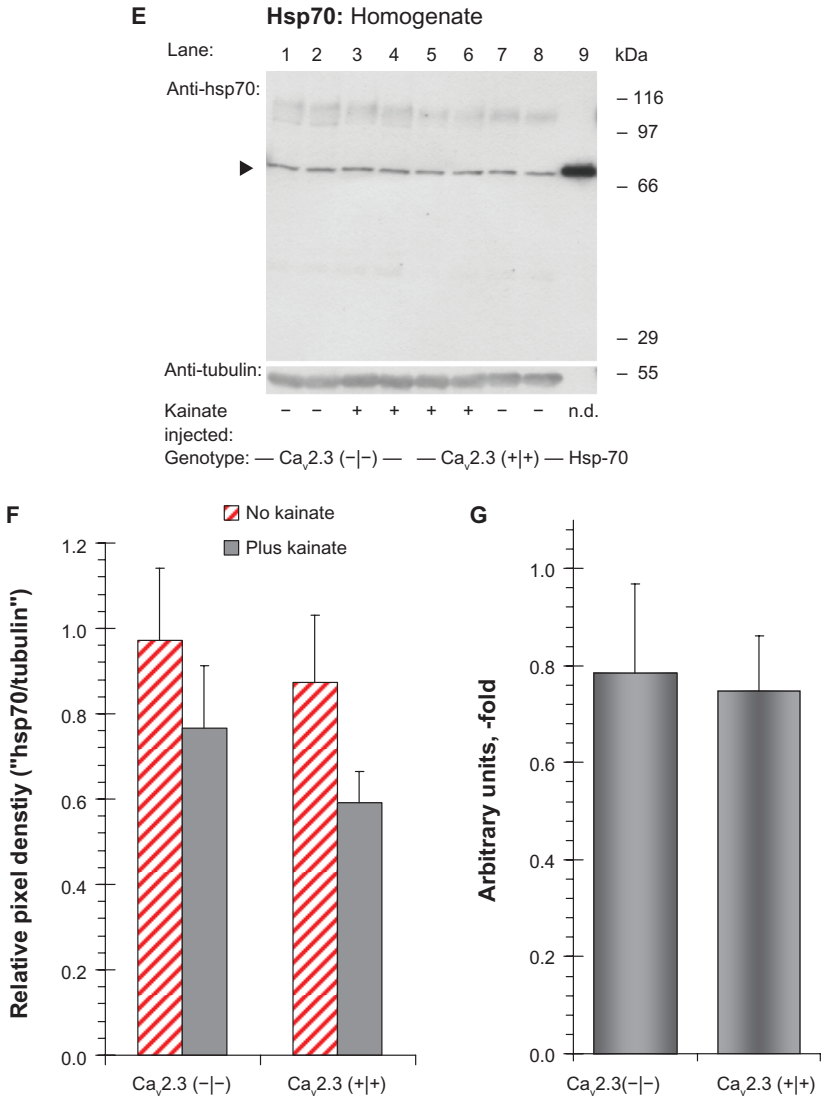


**Figure 3** The membrane-bound fraction of Hsp70 is increased upon kainate injection only in Ca$_v$2.3 controls but not in Ca$_v$2.3-deficient mice. Hsp70 was detected and quantified in microsomal hippocampal membrane fractions from both genotypes. **A**) A monoclonal antibody raised against native human Hsp70 protein was used for detection of membrane-bound Hsp70 from hippocampal tissue of Ca$_v$2.3 control mice (lanes 1–4). Hippocampal microsomes were isolated by ultracentrifugation from the mice either before kainate injection (lanes 1 and 2, duplicates) or after intraperitoneal injection of kainate 20 mg/kg body weight (lanes 3 and 4, duplicates). Protein 10 µg was loaded in the individual lanes. An aliquot of overexpressed human Hsp70 was used as the reference protein (lane 5). Molecular size markers are loaded on lane 6 as indicated. Note, that nonspecific immunoreactive proteins were detected. The 100 kDa proteins were used as an internal standard to perform normalized quantification of anti-Hsp70 positive protein at 70 kDa. The ratios are plotted in panel C as relative pixel density ("Hsp70/100 kDaP"). **B**) Example of anti-Hsp70 positive bands from one of four Western blots, which were used to calculate mean values as shown in panel C. **C**) Mean values of normalized pixel densities from the densitograms shown in panel B. Relative pixel density before (striated box) and after kainate injection (filled box) was determined in six Western blots from two different microsomal membrane batches. **D**) Relative ratio of Hsp70 increase in Ca$_v$2.3-deficient and control mice, which was determined by dividing relative pixel densities after kainate injection by relative density before kainate injection. For Ca$_v$2.3-deficient mice, the ratio is close to 1, revealing no significant increase by kainate injection. The ratio was significantly increased for Ca$_v$2.3 control mice. **E**) The same monoclonal antibody as used in panel A against native human Hsp70 protein was used for the detection of total Hsp70 from hippocampal homogenates of Ca$_v$2.3-deficient (lanes 1–4) and control mice (lanes 5–8). Recombinant Hsp70 was used as a reference (lane 9). The soluble protein fraction from hippocampal tissue was isolated from mice either before kainate injection (duplicates: lanes 1 and 2 vs lanes 7 and 8) or after intraperitoneal injection of kainate 20 mg/kg body weight (lanes 3 and 4 vs lanes 5 and 6). **F**) Mean values of normalized pixel densities from the densitograms shown in panel E, using tubulin as the loading control. Relative pixel density before (striated box) and after kainate injection (filled box) was determined in three Western blots for three different microsomal membrane batches. **G**) Relative ratio of Hsp70 in Ca$_v$2.3-deficient and control mice, which was determined by dividing relative pixel densities after kainate injection by relative density before kainate injection.
**Abbreviation:** Hsp70, heat shock 70 kDa protein 1A.

$P = 0.29$) was not increased significantly, but for Ca$_v$2.3 control mice was significantly raised by 3.3-fold ($1.36 \pm 0.26$, n = 11, $P = 0.013$, Figures 3C and 3D), although in whole tissue homogenates no genotype-specific difference was observed (Figures 3E–G).

## Discussion

During chaperone-mediated protection against neurodegeneration of vulnerable neurons, Hsp70 is considered to be an important partner and signaling intermediate.[31,32] Such a neuroprotective role has been described for several molecular

**Table 1** Comparison of microsomal-bound Hsp70 before and 1 day after injection of 20 µg/g kainate. Male mice at the age of 12–14 weeks were used for the isolation of microsomal membranes from hippocampus. Microsomes were by isolated ultracentrifugation before and 1 day after kainate-injection

| Western blot | Exposition time | Ratios of normalized pixel densities (after/before kainate) | |
|---|---|---|---|
| **Number** | | **$Ca_v2.3$(−\|−)** | **$Ca_v2.3$(+\|+)** |
| 1 | 20 seconds | 1.10 | 4.43 |
| 2 | 1 minute | 0.75 | 3.07 |
| 3 | 2 minutes | 1.36 | 2.00 |
| 4 | 1 minute | 0.99 | 3.31 |
| | Mean | 1.049 | 3.203 |
| | Standard deviation | 0.252 | 0.998 |
| | SEM | 0.126 | 0.499 |
| | n | 4 | 4 |
| | Student's *t*-test, *P*-value | | 0.006 |

chaperones in amyotrophic lateral sclerosis, Alzheimer's disease, Parkinson's disease, and polyglutamine diseases.[16,33] However, more recently, chaperone-assisted degradation has been defined also as an important molecular mechanism in mammalian cells, which facilitates the sorting of non-native proteins to the proteasome and the lysosomal compartment for disposal.[34]

More recently, a histochemical study of Hsp70 expression in brain tissue from patients with temporal lobe epilepsy combined its results with data derived from a rat epilepsy model of kainate-induced cytotoxicity, and defined a somewhat different role for Hsp70, in the sense that Hsp70 may act as a useful indicator of stressed neurons in the acute phase of epilepsy, but may not play an important role in neuroprotection during an epileptogenic state.[12] Because $Ca_v2.3$ inactivation in mice proved to be a useful animal model for convulsive and nonconvulsive seizures, and because Hsp70 interacts with $Ca_v2.3$,[9] we analyzed in more detail if 15-deoxyspergualin, an Hsp70-binding immunosuppressant, may interfere with Hsp70 binding to the cytosolic II–III linker, if Tat-Hsp70, a membrane-penetrating form of Hsp70, may modulate the kinetics of full-length $Ca_v2.3$ $Ca^{2+}$ channels, and if Hsp70 binding to hippocampal microsomal membranes may be changed after kainate injection in control mice, but not in their $Ca_v2.3$-deficient counterparts.

The II–III loops of VGGCs are structurally highly divergent (Figure 4). Within the 450 amino acid-long protein sequence, only the first and the last approximately 100 amino acids align well with the human $Ca_v2.3$ stretch, at least for the three members from the $Ca_v2$ subfamily of non-L-type $Ca^{2+}$ channels. N- ($Ca_v2.2$) and P-/Q-type ($Ca_v2.1$) sequences show about 50% and 40% structural similarity, respectively, in both areas (Figure 4A). Within the II–III loop shown, splice variants of $Ca_v2.3$ differ by an arginine-rich segment which confers a unique $Ca^{2+}$sensitivity to the major neuronal $Ca_v2.3$ splice variants.[24,25,35] Such a segment is absent in $Ca_v2.2$ N-type VGGCs (Figure 4B), and therefore may not be necessary for the binding of Hsp70, as was also shown for the endocrine/cardiac splice variant of $Ca_v2.3$ lacking the arginine-rich segment.[9] Interaction of Hsp70 with the isolated II–III linker of $Ca_v2.2$ seems reasonable, and may also be possible for the II–III linker from Cav2.1, based on the structural similarity

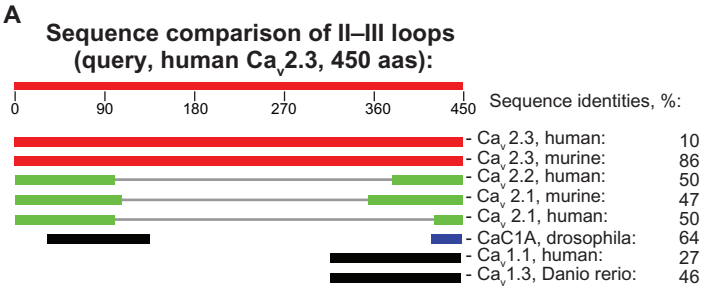


**B Sequence alignment of human E-type ($Ca_v2.3$) and N-type ($Ca_v2.2$) II–III loop:**

```
                                                  Exon 19
Cav2.3    1   DNLANAQELTKDEQEEEEAFNQKHALQKAKEV---SPMSAPNMPSIERDRRRRHHMSMWEPRSSHLRERRRRHHMSVWEQRTSQLRKHMQMSSQEALNREEAP 100
              DNLANAQELTKDE+E EEA NQK ALQKAKEV   SPMSA N+                   S  R++      SVWEQR SQLR     +SE AL  E  P
Cav2.2  710   DNLANAQELTKDEEEMEEAANQKLALQKAKEVAEVSPMSAANI-------------------SIAARQQNSAKARSVWEQRASQLRLQNLRASCEALYSEMDP 793
Cav2.3  380   STVVHISNKTDGEASPLKEAEI-------REDEEEVEKKKQKKEKRETG-KAMVPHSSMFIFSTTNPIRRACHYIVNLR 450
              +T+VHI     G   PL EA +        E + E +K+ +  +   +G + +VP+SSMF  S TN +RR CHYIV +R
Cav2.2 1075   NTIVHIPVMLTG---PLGEATVVPSGNVDLESQAEGKKEVEADDVMRSGPRPIVPYSSMFCLSPTNLLRRFCHYIVTMR 1150
```

**Figure 4** Amino acid sequence alignment of the cytosolic linker between domains II and III (II–III linker) of human $Ca_v2.3$ with the II–III loop of other voltage-gated $Ca^{2+}$ channels. **A)** Left panel: simplified diagram for the regions which aligned with the human $Ca_v2.3$ segment. Right table: Sequence identities were calculated by the BLASTP program, version 2.2.19+.[50,51] **B)** Alignment of the II–III loop sequence from $Ca_v2.3$ and $Ca_v2.2$. Sequence identities are labeled by repeating the identical amino acid in between both sequences. Sequence similarities are labeled by a "+" sign in between both sequences. Note, the exon 19 encoded arginine-rich segment (bold and underlined) is absent in $Ca_v2.2$.

found. Hsp70 binding to the $Ca_v2.2$ loop (and perhaps also to the $Ca_v2.1$ loop) may partially explain why hippocampal microsomes from $Ca_v2.3$-deficient mice also bind Hsp70 to some extent after isolation by ultracentrifugation.

### Tat-Hsp70 modulates $I_{Ca}$ in HEK-293 (2C6) cells stably transfected with $Ca_v2.3$

Preincubation of HEK-293 (2C6) cells with Tat-Hsp70 changed current kinetics moderately, assuming that endogenous Hsp70 had nearly saturated $Ca_v2.3$ binding when using the native charge carrier $Ca^{2+}$ at a concentration of 5 mM. However, even under these conditions, a significant hyperpolarizing shift was observed for the voltage-dependence of activation, as well as a tendency in the same direction for the voltage-dependence of inactivation. Based on these observations, it may be assumed that Hsp70, as a signaling interaction partner, also performs a feedback control to the $Ca_v2.3$ $Ca^{2+}$ channel upon its association with the II–III linker, which is supported by the observation that Tat-Hsp70 reduces the speed of inactivation significantly at early (100 milliseconds) time points. This finding is in accordance with the opposite effect of 15-deoxyspergualin on inactivation,[9] assuming that 15-deoxyspergualin interferes functionally with Hsp70 signaling to $Ca_v2.3$.

The minor changes observed in the kinetic parameters of the $Ca_v2.3$-mediated inward current may have important consequences. For the electrical or chemical stimulation of sustained gamma oscillations or epileptiform burst activity, only minor changes in the balance between excitatory and inhibitory neurotransmission are sufficient to alter the oscillatory frequency or may even result in hypersynchronization of hippocampal activity and lead subsequently to status epilepticus.[30]

### Membrane-bound Hsp70 after kainate injection

Hsp70 chaperones are found in most cellular compartments,[16] where they are localized in the cytosol. Human colon and pancreas carcinoma cell lines,[36] as well as human tumors,[37] differ from normal tissues in their capacity to present Hsp70 on their plasma membrane. The mechanisms for induction of apoptosis may be different in tumor cells, which are lysed by natural killer cells, than in stressed neurons, in which intracellular signaling influences apoptosis and finally neurodegeneration after kainate injection in control mice. Because only a minor part of total cellular Hsp70 associates with membrane fractions in tumors and in hippocampal microsomes, it will be easier to quantify small differences in Hsp70 expression, if one isolates microsomal membranes first, as was done in the present investigation by ultracentrifugation.

Five subunits of kainate receptors are expressed in hippocampal tissue, with region-specific functions.[38,39] In the healthy brain, kainate receptors contribute to normal synaptic transmission and network function, leading to hippocampal and neocortical γ oscillations (20–80 Hz), which play an important role in learning, memory, and cognition. In the pathological brain, kainate receptors are involved in experimentally induced epileptic seizures, finally leading to status epilepticus.[30,40] The network of hippocampal CA3 neurons is mainly affected by kainate receptor activation, where GluR6, the high-affinity kainate receptor, represents the most important target. Kainate receptors are expressed not only postsynaptically but also presynaptically, and knockout mice lacking GluR6 are less susceptible to kainate-induced epilepsy. Further, they perform a reduced frequency facilitation of mossy fiber-mediated excitatory postsynaptic currents (EPSCs).[40] Similarly, $Ca_v2.3$ in the mossy fiber/CA3-synapse has been found to be related to long-term potentiation processes.[41] The detailed pathways of signaling from presynaptic kainate receptors to $Ca_v2.3$ are still unknown. However, the present study gives some evidence for the biochemical interaction of $Ca_v2.3$ with Hsp70 in vivo. When we quantified the total amount of Hsp-70 in homogenates from the hippocampus, no difference was found between either genotypes (Figures 3E–3G). This corresponds to our results from a transcriptome analysis, in which no significant increase in Hsp70 transcripts were identified. However, when we quantified the amount of Hsp70 in microsomal fractions from the hippocampus, which represents a valid fraction for integral membrane proteins, Hsp70 was significantly increased only in control mice, but not in $Ca_v2.3$-deficient mice, suggesting that Hsp70 signaling after kainate injection mainly occurs through $Ca_v2.3$, which binds to Hsp70, and may activate downstream targets related to neurodegenerative processes. This three-fold increase in Hsp70 binding to membrane fractions in mice 1 day after kainate injection is consistent with findings for the rat hippocampus.[12]

If a shift of Hsp70 to the membrane fraction is included in kainate-induced signaling, it may cause overexcitation at mossy fiber/CA3 synapses, leading to increased glutamate release and to neurodegeneration in the CA3 pyramidal neurons. However, if the assumed $Ca_v2.3$-Hsp70 complex is formed within the CA3 neurons, one would need to consider additional candidates for the downstream signaling, as reported in the literature. The most important interaction partner of Hsp70 in the context of apoptosis

and neurodegeneration is the cochaperone, CHIP (carboxy terminus of Hsp70-interacting protein), which is closely involved in aggresome formation.[42,43] Through its binding to Hsp70, CHIP may be involved in the molecular machinery controlling aggresome formation and subsequent elimination of misfolded and aggregated proteins. CHIP deficiency in mice reduces their lifespan, along with an accelerated age-related pathophysiological phenotype.[44]

Interestingly, CHIP, as well as Hsp70 (Hsp72), interacts with apoptosis signal-regulating kinase 1 (ASK1), and prevents apoptosis.[45,46] It has been shown that the anti-apoptotic effect of CHIP is mediated via induction of ubiquitinylation and subsequent degradation of ASK1.[45] ASK1 is a serine-threonine protein kinase which acts as a mitogen-activated protein kinase kinase kinase (MAPKKK) to activate the c-Jun N-terminal kinase and p38 MAPK signaling cascades.[45,47] Multiple steps, including self-dimerization, phosphorylation, and protein–protein interactions, regulate the activity of ASK1. Hsp70 (Hsp72) binds ASK1 at its amino terminus and inhibits the ASK1 dimerization induced by thermal stress.[46]

Interestingly, expression profiling of HEK-293 (2C6) cells stably transfected with $Ca_v2.3$ compared with non-transfected HEK-293 cells revealed the highest increase in expression level to be for mitogen-activated protein kinase kinase 5 (MAP2 K5),[48] which favors involvement of MAP kinase pathways in $Ca_v2.3$-Hsp70-mediated signaling.

An alternate route for signaling could be in the opposite direction, ie, from Hsp70 to $Ca_v2.3$, as indicated by the already mentioned "feedback" of Hsp70 on $Ca_v2.3$. In the event of forward directed signaling from the kainate receptor to Hsp70 and $Ca_v2.3$, a slight shift in the threshold of activation for $Ca_v2.3$ may increase the $Ca^{2+}$ influx at lower membrane potentials, and could activate $Ca^{2+}$-dependent proteases known to be involved in neurodegeneration, as has been shown for calpain after calpastatin depletion in Alzheimer's disease.[49]

Whatever will be the correct explanation for the observed differences between $Ca_v2.3$ control and $Ca_v2.3$-deficient mice after kainate injection and subsequent neurodegeneration, increased Hsp70 binding to microsomal membranes represents an important (albeit only an intermediate) step leading finally via other processes to hippocampal neurodegeneration after kainate injection, similar to what has been reported for the rat hippocampus.[12] Therefore, using the kainate model for both control and $Ca_v2.3$-deficient mice will help in future to elucidate in detail the molecular steps involved in kainate-induced and $Ca_v2.3$-mediated neuronal cell death.

## Acknowledgments

Our research was supported by the Center of Molecular Medicine Cologne. We are grateful to Ms Renate Clemens for her excellent technical assistance, and to Dr Dr Marco Weiergräber for his continuous support and critical discussions.

## Disclosure

The authors report no conflicts of interest in this work.

## References

1. Ertel EA, Campbell KP, Harpold MM, et al. Nomenclature of voltage-gated calcium channels. *Neuron*. 2000;25:533–535.
2. Catterall WA, Few AP. Calcium channel regulation and presynaptic plasticity. *Neuron*. 2008;59:882–901.
3. Striessnig J, Koschak A. Exploring the function and pharmacotherapeutic potential of voltage-gated $Ca^{2+}$ channels with gene knockout models. *Channels (Austin)*. 2008;2:233–251.
4. Kamp MA, Krieger A, Henry M, Hescheler J, Weiergräber M, Schneider T. Presynaptic "Cav2.3 containing" E-type $Ca^{2+}$ channels share dual roles during neurotransmitter release. *Eur J Neurosci*. 2005; 21:1617–1625.
5. Weiergräber M, Kamp MA, Radhakrishnan K, Hescheler J, Schneider T. The Cav2.3 voltage-gated calcium channel in epileptogenesis. Shedding new light on an enigmatic channel. *Neurosci Biobehav Rev*. 2006;30: 1122–1144.
6. Weiergräber M, Henry M, Ho MSP, Struck H, Hescheler J, Schneider T. Altered thalamocortical rhythmicity in Cav2.3-deficient mice. *Mol Cell Neurosci*. 2008;39:605–618.
7. Weiergräber M, Henry M, Krieger A, et al. Altered seizure susceptibility in mice lacking the Cav2.3 E-type $Ca^{2+}$ channel. *Epilepsia*. 2006;47: 839–850.
8. Weiergräber M, Henry M, Radhakrishnan K, Hescheler J, Schneider T. Hippocampal seizure resistance and reduced neuronal excitotoxicity in mice lacking the Cav 2.3 E/R-type voltage-gated calcium channel. *J Neurophysiol*. 2007;97:3660–3669.
9. Krieger A, Radhakrishnan K, Pereverzev A, et al. The molecular chaperone Hsp70 interacts with the cytosolic II-III loop of the Cav2.3 E-type voltage-gated $Ca^{2+}$ channel. *Cell Physiol Biochem*. 2006;17: 97–110.
10. Lindquist S. The heat-shock response. *Annu Rev Biochem*. 1986;55: 1151–1191.
11. Elia G, Santoro MG. Regulation of heat shock protein synthesis by quercetin in human erythroleukaemia cells. *Biochem J*. 1994; 300(Pt 1):201–209.
12. Yang T, Hsu C, Liao W, Chuang JS. Heat shock protein 70 expression in epilepsy suggests stress rather than protection. *Acta Neuropathol*. 2008;115:219–230.
13. Miltiadous P, Stamatakis A, Stylianopoulou F. Neuroprotective effects of IGF-I following kainic acid-induced hippocampal degeneration in the rat. *Cell Mol Neurobiol*. 2010;30:347–360.
14. Blondeau N, Plamondon H, Richelme C, Heurteaux C, Lazdunski M. K(ATP) channel openers, adenosine agonists and epileptic preconditioning are stress signals inducing hippocampal neuroprotection. *Neuroscience*. 2000;100:465–474.
15. Radhakrishnan K, Hescheler J, Schneider T. Heat shock proteins and ion channels. Functional interactions and therapeutic consequences. *Curr Pharm Biotechnol*. 2010;11:175–179.
16. Muchowski PJ, Wacker JL. Modulation of neurodegeneration by molecular chaperones. *Nat Rev Neurosci*. 2005;6:11–22.
17. Krueger AM, Armstrong JN, Plumier J, Robertson HA, Currie RW. Cell specific expression of Hsp70 in neurons and glia of the rat hippocampus after hyperthermia and kainic acid-induced seizure activity. *Brain Res Mol Brain Res*. 1999;71:265–278.

18. Voisine C, Pedersen JS, Morimoto RI. Chaperone networks: Tipping the balance in protein folding diseases. *Neurobiol Dis*. 2010;40:12–20.
19. Schneider T, Wei X, Olcese R, et al. Molecular analysis and functional expression of the human type E a1 subunit. *Receptors Channels*. 1994;2:255–270.
20. Mehrke G, Pereverzev A, Grabsch H, Hescheler J, Schneider T. Receptor mediated modulation of recombinant neuronal class E calcium channels. *FEBS Lett*. 1997;408:261–270.
21. Dietz GPH, Bähr M. Synthesis of cell-penetrating peptides and their application in neurobiology. *Methods Mol Biol*. 2007;399:181–198.
22. Nagel F, Dohm CP, Bähr M, Wouters FS, Dietz GPH. Quantitative evaluation of chaperone activity and neuroprotection by different preparations of a cell-penetrating Hsp70. *J Neurosci Methods*. 2008; 171:226–232.
23. Pereverzev A, Klöckner U, Henry M, et al. Structural diversity of the voltage-dependent $Ca^{2+}$ channel a1E subunit. *Eur J Neurosci*. 1998;10: 916–925.
24. Leroy J, Pereverzev A, Vajna R, et al. $Ca^{2+}$-sensitive regulation of E-type $Ca^{2+}$ channel activity depends on an arginine rich region in the cytosolic II–III loop. *Eur J Neurosci*. 2003;18:841–855.
25. Klöckner U, Pereverzev A, Leroy J, et al. The cytosolic II–III loop of Cav2.3 provides an essential determinant for the phorbol ester-mediated stimulation of E-type $Ca^{2+}$ channel activity. *Eur J Neurosci*. 2004;19: 2659–2668.
26. Siapich SA, Banat M, Albanna W, Hescheler J, Lüke M, Schneider T. Antagonists of ionotropic gamma-aminobutyric acid receptors impair the $NiCl_2$-mediated stimulation of the electroretinogram B-wave amplitude from the isolated superfused vertebrate retina. *Acta Ophthalmol*. 2009;87:854–865.
27. Dietz GPH, Bähr M. Peptide-enhanced cellular internalization of proteins in neuroscience. *Brain Res Bull*. 2005;68:103–114.
28. Nakashima YM, Todorovic SM, Pereverzev A, Hescheler J, Schneider T, Lingle CJ. Properties of $Ba^{2+}$ currents arising from human a1E and a1Eb3 constructs expressed in HEK293 cells: Physiology, pharmacology, and comparison to native T-type $Ba^{2+}$ currents. *Neuropharmacology*. 1998;37:957–972.
29. Nadler JV, Perry BW, Cotman CW. Intraventricular kainic acid preferentially destroys hippocampal pyramidal cells. *Nature*. 1978;271: 676–677.
30. Fisahn A. Kainate receptors and rhythmic activity in neuronal networks: Hippocampal gamma oscillations as a tool. *J Physiol*. 2005;562: 65–72.
31. Ranford JC, Coates AR, Henderson B. Chaperonins are cell-signalling proteins: The unfolding biology of molecular chaperones. *Expert Rev Mol Med*. 2000;2:1–17.
32. Stankiewicz AR, Lachapelle G, Foo CP, Radicioni SM, Mosser DD. Hsp70 inhibits heat-induced apoptosis upstream of mitochondria by preventing Bax translocation. *J Biol Chem*. 2005;280:38729–38739.
33. Meriin AB, Sherman MY. Role of molecular chaperones in neurodegenerative disorders. *Int J Hyperthermia*. 2005;21:403–419.
34. Kettern N, Dreiseidler M, Tawo R, Hohfeld J. Chaperone-assisted degradation: Multiple paths to destruction. *Biol Chem*. 2010;391: 481–489.
35. Pereverzev A, Leroy J, Krieger A, et al. Alternate splicing in the cytosolic II-III loop and the carboxy terminus of human E-type voltage-gated $Ca^{2+}$ channels: Electrophysiological characterization of isoforms. *Mol Cell Neurosci*. 2002;21:352–365.
36. Gross C, Koelch W, DeMaio A, Arispe N, Multhoff G. Cell surface-bound heat shock protein 70 (Hsp70) mediates perforin-independent apoptosis by specific binding and uptake of granzyme B. *J Biol Chem*. 2003;278:41173–41181.
37. Gehrmann M, Liebisch G, Schmitz G, et al. Tumor-specific Hsp70 plasma membrane localization is enabled by the glycosphingolipid Gb3. *PLoS One*. 2008;3:e1925.
38. Wisden W, Seeburg PH. A complex mosaic of high-affinity kainate receptors in rat brain. *J Neurosci*. 1993;13:3582–3598.
39. Schoepfer R, Monyer H, Sommer B, et al. Molecular biology of glutamate receptors. *Prog Neurobiol*. 1994;42:353–357.
40. Pinheiro P, Mulle C. Kainate receptors. *Cell Tissue Res*. 2006;326: 457–482.
41. Dietrich D, Kirschstein T, Kukley M, et al. Functional specialization of presynaptic Cav2.3 $Ca^{2+}$ channels. *Neuron*. 2003;39:483–496.
42. Olzmann JA, Li L, Chin LS. Aggresome formation and neurodegenerative diseases: therapeutic implications. *Curr Med Chem*. 2008;15:47–60.
43. Sha Y, Pandit L, Zeng S, Eissa NT. A critical role for CHIP in the aggresome pathway. *Mol Cell Biol*. 2009;29:116–128.
44. Min JN, Whaley RA, Sharpless NE, Lockyer P, Portbury AL, Patterson C. CHIP deficiency decreases longevity, with accelerated aging phenotypes accompanied by altered protein quality control. *Mol Cell Biol*. 2008;28:4018–4025.
45. Hwang JR, Zhang C, Patterson C. C-terminus of heat shock protein 70-interacting protein facilitates degradation of apoptosis signal-regulating kinase 1 and inhibits apoptosis signal-regulating kinase 1-dependent apoptosis. *Cell Stress Chaperones*. 2005;10:147–156.
46. Park HS, Cho SG, Kim CK, et al. Heat shock protein Hsp72 is a negative regulator of apoptosis signal-regulating kinase 1. *Mol Cell Biol*. 2002;22:7721–7730.
47. Takeda K, Noguchi T, Naguro I, Ichijo H. Apoptosis signal-regulating kinase 1 in stress and immune response. *Annu Rev Pharmacol Toxicol*. 2008;48:199–125.
48. Natrajan R, Little SE, Reis-Filho JS, et al. Amplification and overexpression of CACNA1E correlates with relapse in favorable histology Wilms' tumors. *Clin Cancer Res*. 2006;12:7284–7293.
49. Rao MV, Mohan PS, Peterhoff CM, et al. Marked calpastatin (CAST) depletion in Alzheimer's disease accelerates cytoskeleton disruption and neurodegeneration: Neuroprotection by CAST overexpression. *J Neurosci*. 2008;28:12241–12254.
50. Altschul SF, Madden TL, Schäffer AA, et al. Gapped BLAST and PSI-BLAST: A new generation of protein database search programs. *Nucleic Acids Res*. 1997;25:3389–3402.
51. Altschul SF, Wootton JC, Gertz EM, et al. Protein database searches using compositionally adjusted substitution matrices. *FEBS J*. 2005;272: 5101–5109.



**Journal of Receptor, Ligand and Channel Research**

Dovepress

## Publish your work in this journal

The Journal of Receptor, Ligand and Channel Research is an international, peer-reviewed, open access, online journal. The journal welcomes laboratory and clinical findings in the fields of biological receptors, ligands, channel and signal transduction research including: receptors and signalling; ligands; transporters, pores and channels; binding and activation; receptor regulation; role of receptors in diseases and their treatment; molecular basis of membrane structure and functions; molecular models of membranes. The manuscript management system is completely online and includes a very quick and fair peer-review system. Visit http://www.dovepress.com/testimonials.php to read real quotes from published authors.

**Submit your manuscript here:** http://www.dovepress.com/journal-of-receptor-ligand-and-channel-research-journal